



## Backbone assignment of HMGB1 A-box and molecular interaction with Hoxc9DBD studied by paramagnetic probe

Ji Woong Choi and Sung Jean Park\*

College of Pharmacy and Gachon Institute of Pharmaceutical Sciences, Gachon University, 191 Hambakmo-ero, Yeonsu-gu, Incheon 21936, Korea

Received May 28, 2021; Revised June 7, 2021; Accepted June 7, 2021

**Abstract** High mobility group protein B1 (HMGB1) is a highly conserved, non-histone, chromatin associated nuclear protein encoded by HMGB1 gene. HMGB1 proteins may be general co-factors in Hox-mediated transcriptional activation that facilitate the access of Hox proteins to specific DNA targets. It is unclear that the exact binding interface of Hoxc9DBD and HMGB1. To identify the interface and binding affinity of Hoxc9DBD and HMGB1 A-box, the paramagnetic probe, MTSL was used in NMR titration experiment. It is attached to the N-terminal end of HMGB1 A-box by reaction with thiol groups. The backbone assignment of HMGB1 A-box was achieved with 3D NMR techniques. The <sup>15</sup>N-labeled HMGB1 A-box was titrated with MTSL-labeled Hoxc9DBD respectively. Based on the chemical shift changes we can identify the interacting residues and further map out the binding sites on the protein structure. The NMR titration result showed that the binding interface of HMGB1 A-box is around loop-1 between helix-1 and helix-2. In addition, the additional contacts were found in N- and C-terminus. The N-terminal arm region of Hoxc9DBD is the major binding region and the loop between helix1 and helix2 is the minor binding region.

**Keywords** Backbone assignment, HMGB1, Hoxc9, Paramagnetic probe

### Introduction

Human HMGB1 has 215 amino acids and consists of two DNA binding domains (named by A box and B box) and an acidic C-terminal tail.<sup>1</sup> The two DNA binding domains both formed an similar L- shaped structure that comprised of two short  $\alpha$ -helix and a long  $\alpha$ -helix.<sup>2</sup> HMGB1 regulates the transcription factors and pervious study showed that it is necessary for the interaction between HMGB1 and transcription factors. The important part between the protein interactions is thought to be the HMGB1 A-box and B-box. HMG A-box and B-box are about 30% identical in amino acid sequence.<sup>3</sup> Though the structures are similar of A and B box, A-box has a higher preference for distorted DNA and B-box is more effective at bending linear DNA.<sup>4-6</sup> A-box functions as protein chaperone roles and B-box functions as DNA chaperone roles.<sup>7</sup> HMGB1 is known as a co factor structural significant for proper transcriptional regulation in somatic cells.<sup>8</sup> When HMGB1 interacts with transcription factors, it could bend DNA and let transcription factors more access to its target DNA binding site. The distorted DNA could be a more favorable conformation for the transcription factor to bind.<sup>9</sup> HMG proteins also have been shown to facilitate the sequence-specific DNA binding of a large amount of transcription factors such as sex-hormone receptor,<sup>10,11</sup> Hox proteins,<sup>12</sup> POU domain-

\* Address correspondence to: **Sung Jean Park**, College of Pharmacy and Gachon Institute of Pharmaceutical Sciences, Gachon University, 191 Hambakmo-ero, Yeonsu-gu, Incheon 21936, Korea Tel: 82-32-820-4957; E-mail: psjn mr@gachon.ac.kr

containing factors,<sup>13</sup> and p53, functioning as a coactivator for transcription of their target genes.<sup>14</sup> For example, HMGB1 functions as a cofactor activator of p53, a tumor suppressor protein.<sup>3</sup> The physical interaction between HMGB1 and p53 has been investigated. The interaction with p53 may induce the conformational change in HMGB1 A-box that optimizes DNA binding by HMGB1.<sup>3</sup> HMGB1 as a conserved non-histone nuclear protein has been involved in a variety of biological processes of cancer, such as cell proliferation, apoptosis, autophagy, angiogenesis and metastasis.<sup>15</sup> Autophagy functions as a cell survival mechanism to promote cancer progression in certain circumstances.<sup>16,17</sup> HMGB1 overexpression is widespread in large amount of cancers, such as HMGB1 expression was significantly increased in bladder cancer tissues.<sup>18</sup> Previously, HMG-box proteins can stimulate the binding of sequence-specific DNA-binding proteins bind to their target DNA.<sup>9</sup> Hox homeodomain interacts with single A and B HMG boxes of HMGB1. HMG proteins could increase the transcription of Hox proteins in vivo.<sup>12</sup> Therefore, HMGB1 proteins may be general co-factors in Hox-mediated transcriptional activation that facilitate the access of Hox proteins to specific DNA targets and introduce architectural constraints in the assembly of Hox-containing transcriptional complexes.<sup>12</sup> The three dimensional (3D) structures of HMGB1 A-box and Hoxc9DBD have been already determined.<sup>19,20</sup> However it is still unclear that which residues are directly involved in the interaction and how strong of the binding. To better understand the mechanisms of Hoxc9DBD-HMGB1 A-box interactions, NMR titration with the paramagnetic probe, MTSL (S-(1-oxyl-2,2,5,5-tetramethyl-2,5-dihydro-1H-pyrrol-3-yl)methyl methanesulfonylthioate) was performed in the present study.

## Experimental Methods

**Sample preparation-** The gene encoding HMGB1 A-box domain was cloned into the pGEX4T-2 vector at

the BamHI and XhoI sites. *E.coli* BL21 cells bearing the HMGB1A-box expression vector were grown in LB media at 37 degree until OD<sub>600</sub> was 0.6, and then add isopropyl-β-D-1-thiogalactopyranoside (IPTG) to a final concentration of 0.5 mM. Cells were harvested 4 h after induction at 37°C. Harvested, sonicated the cells and removed the cell debris using centrifugation. The GST-tagged protein was purified by a GST-affinity column that is GSTPrep™ FF 16/60 (GE Healthcare) and followed by cation exchange chromatography with HiTrap™ SP HP (GE healthcare) and gel filtration chromatography with Hiprep 26/60 sephacryl S100 (GE healthcare). To prepare uniformly <sup>15</sup>N-labeled HMGB1A-box domain and <sup>15</sup>N-labeled Hoxc9DBD, bacterial cells were cultured in M9 minimal medium containing 99% <sup>15</sup>NH<sub>4</sub>Cl (Cambridge isotope laboratories, Inc.) The <sup>15</sup>N-labeled proteins were dissolved in 20 mM sodium phosphate buffer (pH 6.5) containing 10% D<sub>2</sub>O, 50 mM NaCl, and 1 mM EDTA. The gene that encodes human Hoxc9DBD was inserted into the pET28a vector at the NcoI and XhoI sites. The construct was transformed into Resetta2 (DE3) *E.coli*. The *E.coli* cells were grown in luria bertani (LB) media at 37 degree until the OD<sub>600</sub> was 0.5. Add isopropyl-β-D-1-thiogalactopyranoside (IPTG) to a final concentration 0.5 mM, after that transfer cells to 20°C for 16 h. Harvested, sonicated the cells and removed the cell debris using centrifugation. For the purification of Human Hoxc9DBD protein, cation exchange chromatography and gel filtration chromatography were needed. The columns of HiTrap™ SP HP (GE healthcare) and Hiprep 26/60 sephacryl S100 (GE healthcare) were applied.

**Labeling with MTSL-** MTSL was used as paramagnetic probe to paramagnetic protein. MTSL is an organosulfur compound that attach to proteins by reaction with thiol groups. Fivefold molar excess of spin-labeling reagent MTSL was added in protein solution and the MTSL reaction was processed at 4 degree for 12 h. Excess MTSL can be removed by using a desalting column. A subset of HSQC spectrum were gained to monitor the peak position changes of <sup>15</sup>N-labeled HMGB1 A-box in the presence of

increasing molar ratios of unlabeled MTSL-Hoxc9DBD (Fig. 1).

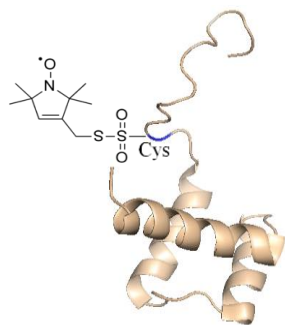


**Figure 1.** The structure of MTSL-Hoxc9DBD. The N-terminal cysteine harbors the MTSL.

*NMR experiments-* Backbone and side chain  $^1\text{H}$ ,  $^{13}\text{C}$  and  $^{15}\text{N}$  resonances for Hoxc9DBD and HMGB1A-

box were assigned based on standard triple-resonance experimental spectra. Sequential assignment of  $^{13}\text{C}$ ,  $^{15}\text{N}$ -labeled proteins was achieved by 3D triple resonance through-bond scalar correlation experiments such as 3D HNCOC, HNCACOC, HNCA, HN(CO)CA, HNCACB, CBCA(CO)NH experiments<sup>21,22</sup> Two dimensional  $^1\text{H}$ ,  $^{15}\text{N}$ -HSQC spectra were recorded on uniformly  $^{15}\text{N}$ -labeled HMGB1A-box in the presence of different concentrations of Hoxc9DBD and MTSL Hoxc9DBD. The chemical shift perturbation between the free-form and bound-form was normalized using the following formula and expressed in ppm:  $\Delta\delta = [0.5 \times (\Delta\delta\text{H})^2 + (\Delta\delta\text{N}/5)^2]^{1/2}$ , where  $\Delta\delta\text{H}$  and  $\Delta\delta\text{N}$  are the differences in the chemical shifts of amide protons and nitrogens between the initial and final data points of the titration, respectively. All NMR experiments were performed at

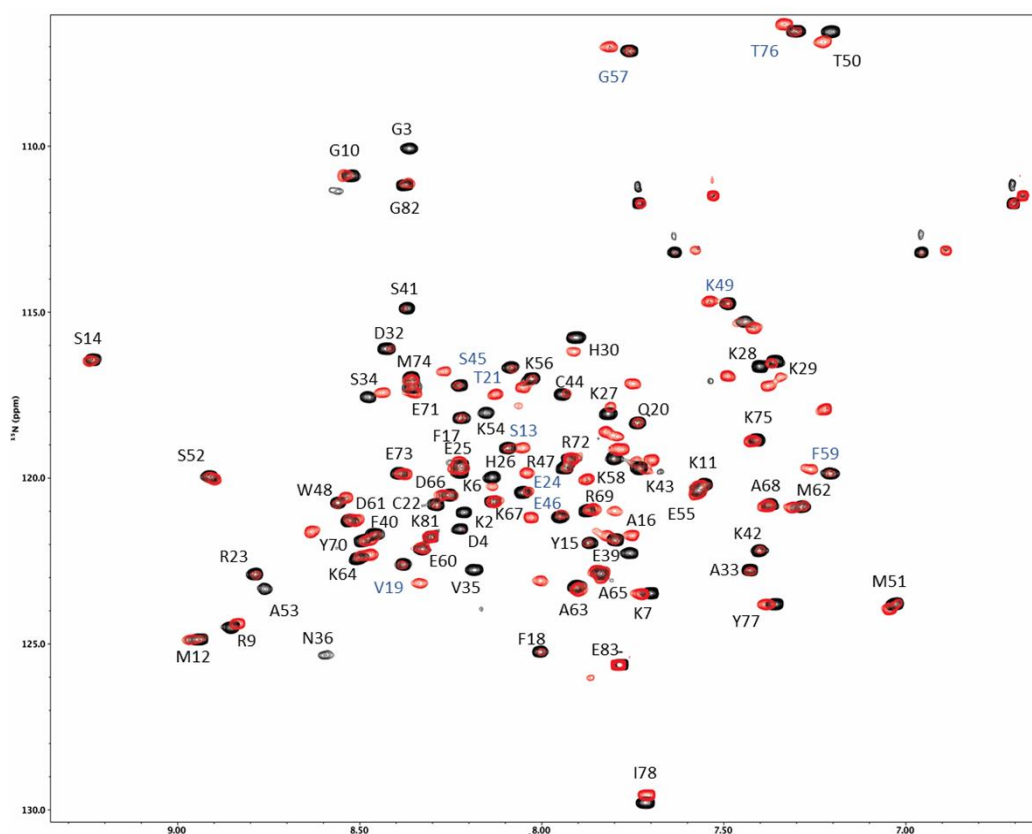


**Figure 2.**  $^1\text{H}$ ,  $^{15}\text{N}$  HSQC spectra of  $^{15}\text{N}$ -labelled HMGB1 A-box at pH 6.5, 298K. The backbone amide cross peaks are annotated by residue names and numbers. The apo protein is colored in black and the 1:1 complex of  $^{15}\text{N}$ -HMGB1 A-box and unlabeled-Hox9DBD is colored in red.

298 K on a Bruker AVANCE DRX 900 and 800 MHz spectrometer equipped with a cryogenic probe. NMR data were processed using NMRPipe and analyzed using NMRView. Protein samples for NMR experiments were prepared in NMR buffer (20 mM sodium phosphate buffer, 50 mM NaCl, and 1 mM EDTA, pH 6.5).

## Results and Discussion

**Backbone assignment of HMGB1 A-box** – . The  $^1\text{H}$ ,  $^{15}\text{N}$ -HSQC spectrum of  $^{15}\text{N}$ -enriched HMGB1 A-box showed well-dispersed cross-peaks, indicating that the overall structure of the HMGB1 A-box is well defined. Most of the  $^1\text{HN}$ ,  $^{15}\text{N}$ ,  $^{13}\text{C}_\alpha$ ,  $^{13}\text{C}_\beta$ , and  $^{13}\text{CO}$  resonance assignments were obtained from analyses of the 3D HNCA, HNCACB, CBCA(CO)NH, HN(CA)CO and HNCOC spectra. Since any one residue manifests the same HN and  $^{15}\text{N}$  chemical shift signals in each spectrum, the related peaks could be combined into a peak cluster. The backbone amide resonances for 83 possible residues were completely assigned, except for those of the isolated prolines. The available resonances is depicted in Figure 2.

**Titration of MTSL-Hoxc9DBD into  $^{15}\text{N}$  HMGB1 A box**– MTSL was used as paramagnetic probe in the present study. It attached to N-terminal cysteine of Hoxc9DBD to form MTSL-Hoxc9DBD protein. In the HSQC spectrum of  $^{15}\text{N}$  HMGB1 A box titrated with

MTSL-Hoxc9DBD, the black peaks are free state HMGB1 A-box and red peaks are free state HMGB1 A-box bound with MTSL-Hoxc9DBD (Fig. 2). The spectrum of  $^{15}\text{N}$  HMGB1 A-box upon binding to MTSL-Hoxc9DBD showed signal change by the binding event as well as relaxation enhancement by paramagnetic probe. Addition of DTT in the protein mixture of MTSL-Hoxc9DBD with  $^{15}\text{N}$  HMGB1 A-box to eliminate the paramagnetic effect and pseudo contact shift caused by MTSL. The dose-dependent shifts are thought to be caused by MTSL and binding between HMGB1 A-box and MTSL-Hoxc9DBD. The residues in the helix1 and helix2 (V19, T21, E24, K29, H30, E39, S45, E46) showed a relatively high chemical shift perturbation (CSP) over 0.0477 upon binding to the MTSL-Hoxc9DBD (Fig. 3). In addition, seven residues (K2, G3, D4, S34, N36, A53 and K54) showed significant intensity reduction upon binding. Next, by comparing two spectra which were obtained before and after addition of DTT in the mixture of MTSL-Hoxc9DBD and  $^{15}\text{N}$  HMGB1 A-box, the relaxation enhancement and pseudo contact shifts caused by MTSL were estimated. In the Figure 4, black peaks are HMGB1 A-box bound with MTSL-Hoxc9DBD with DTT and red peaks are HMGB1 A-box bound to MTSL-Hoxc9DBD without DTT. The intensity changes in the presence and the absence of DTT are also plotted in Figure 4. Among the residues which showing the significant perturbation in Figure 3, K29, H30 were highly affected from paramagnetic effect. In addition, V19, T21, E24, E39, S45, E46 were

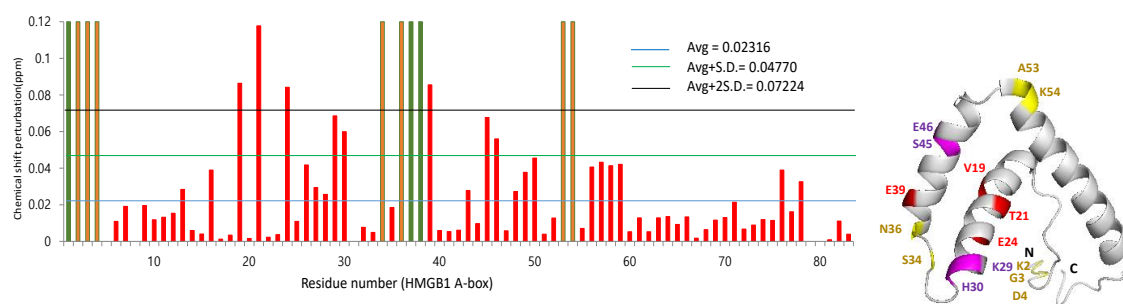


**Figure 3.** A plot of chemical shift perturbation for (Fig. 2) along with the sequence of  $^{15}\text{N}$  HMGB1 A-box is shown. The black line at 0.0722 ppm represents (Avg + 2S.D.), while the blue line at 0.0477 ppm represents (Avg + S.D.) and the green line at 0.0232 ppm represents (Avg). S.D represents standard deviation of the average. The disappeared residues are colored in yellow. Among the peaks moved above (Avg), residues influenced by paramagnetic relaxation enhancement are colored in orange and residues influenced by binding effect are colored in red. The affected residues are depicted on the structure of HMGB1 A-box (PDB ID: 2RTU).

notably changed in the spectrum of Figure 4. Therefore the residues that CSP value above 0.0477 can be divided into two parts. One group is the residues that are highly affected by direct contact between two proteins and the other group is the residues involving V19, T21, E24, E39, S45, and E46 are highly influenced by paramagnetic effect. The

residues, K29 and H30 are influenced by both the binding and paramagnetic effects. The residues that showed intensity perturbation caused by MTSL are mapped on the structures based on the structure (Fig. 4). Using the residues that located on the binding interfaces between HMGB1 A-box and Hoxc9DBD confirmed from first titration result which showed the

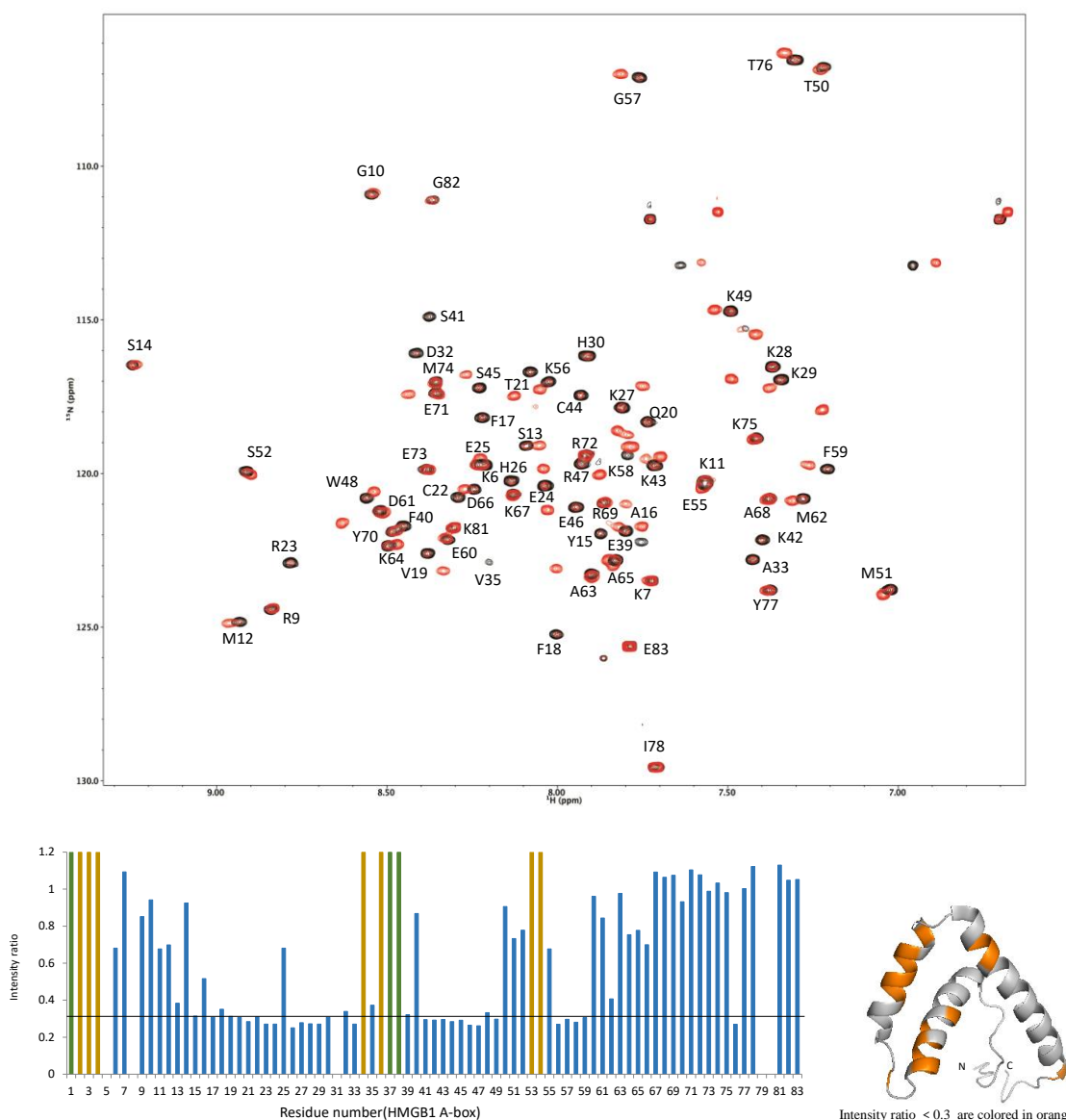


**Figure 4.**  $^1\text{H}$ - $^{15}\text{N}$  HSQC spectra of  $^{15}\text{N}$ -labelled HMGB1 A-box at pH 6.5, 298K.  $^{15}\text{N}$ -HMGB1 A-box upon addition of MTSL-Hoxc9DBD in the presence of DTT (black) and in the absence of DTT (red). A plot of intensity perturbation along with the sequence of  $^{15}\text{N}$  HMGB1 A-box is shown. The green bars represent the unidentified residues in the spectra. The significantly affected residues are depicted on the structure of HMGB1 A-box in orange color (PDB ID: 2RTU).

group Kd value was  $8.77 \pm 3.02 \mu\text{M}$ . The group Kd value was obtained from the titration result of the residues including H26, K27, K28, K29, and H30. Their chemical shift change was fitted to the built-in 1:1 model in NMRView.<sup>23</sup>

## Conclusion

Based on the NMR titration results, the expected complex structure of HMGB1 A-box and Hoxc9DBD (Fig. 5) was obtained. The N terminal arm region of Hoxc9DBD may interact with loop1 of HMGB1 A-

box. In addition, the loop between helix1 and helix2 of Hoxc9DBD may interact with N- and C- terminal of HMGB1 A-box. The MTSL assay was helpful to identify residues located in helix1 and helix2 of HMGB1 A-box that are involved in interaction and was not identified in the normal titration experiment. In this study we identified the residues of Hoxc9DBD and HMGB1 A-box and their binding affinity. These findings may give a clue for targeted therapeutic intervention. Anti-cancer agents can be explored in the help of the interface of Hoxc9DBD and HMGB1 A-box.

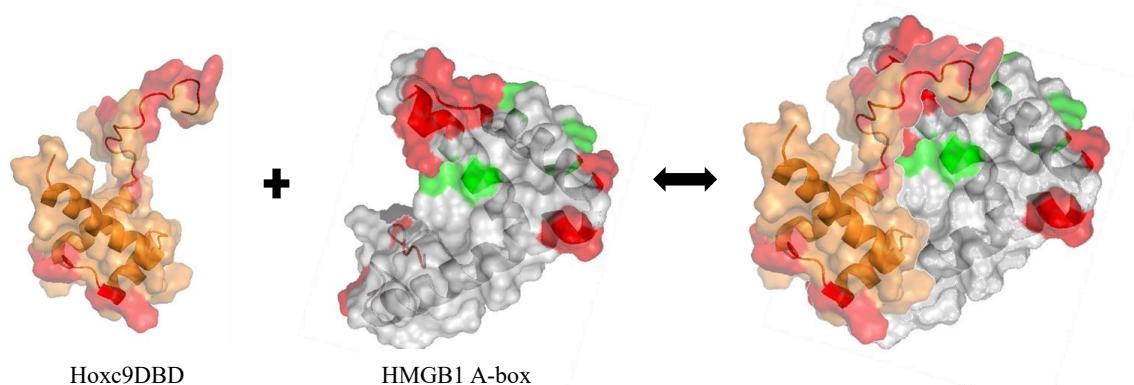


**Figure 5.** The expected complex structure of HMGB1 A box (PDB ID: 2RTU) and Hoxc9DBD (PDB ID: 2MSY)

## Acknowledgements

This work was supported by the Gachon University research fund of 2019 (GCU-2019-0707). This research was also supported by the National Research Foundation of Korea (NRF) funded by the Ministry of Education, Science, and Technology (2018R1D1A1B07050426). The authors thank the high field NMR facility at the Korea Basic Science Institute and the National Center for Inter-university Research Facilities.

## References

1. H. Yang, H. Wang, S. S. Chavan, and U. Andersson, *Mol. Med.* **21**, S6 (2015)
2. M. Sutrias-Grau, M. E. Bianchi, and J. Bernués, *J. Biol. Chem.* **274**, 1628 (1999)
3. T. Imamura, H. Izumi, G. Nagatani, T. Ise, M. Nomoto, Y. Iwamoto, and K. Kohno, *The Journal of Biological Chemistry* **276**, 7534 (2001)
4. M. Webb and J. O. Thomas, *J. Mol. Biol.* **294**, 373 (1999)
5. T. T. Paull, M. J. Haykinson, and R. C. Johnson, *Genes Dev.* **7**, 1521 (1993)
6. S. H. Teo, K. D. Grasser, and J. O. Thomas, *Eur. J. Biochem.* **230**, 943 (1995)

7. J. P. Rowell, K. L. Simpson, K. Stott, M. Watson, and J. O. Thomas, *Structure* **20**, 2014 (2012)
8. M. T. Lotze and K. J. Tracey, *Nat. Rev. Immunol.* **5**, 331 (2005)
9. J. O. Thomas and A. A. Travers, *Trends Biochem. Sci.* **26**, 167 (2001)
10. C. S. Verrier, N. Roodi, C. J. Yee, L. R. Bailey, R. A. Jensen, M. Bustin, and F. F. Parl, *Mol Endocrinol.* **11**, 1009 (1997)
11. S. A. Oñate, P. Prendergast, J. P. Wagner, M. Nissen, R. Reeves, D. E. Pettijohn, and D. P. Edwards, *Mol Cell Biol.* **14**, 3376 (1994)
12. V. Zappavigna et al., *EMBO J.* **15**, 4981 (1996)
13. S. Zwilling, H. König, and T. Wirth, *EMBO J.* **14**, 1198 (1995)
14. L. Jayaraman, N. C. Moorthy, et al., *Genes Dev.* **12**, 462 (1998)
15. C. Pan, Y. Wang, et al., *J. Biol. Regul. Homeost. Agents.* **31**, 41 (2017)
16. W. He, Q. Wang, et al., *Autophagy* **8**, 1811 (2012)
17. M. Kang, C. W. Jeong, et al., *Int. J. Mol. Sci.* **15**, 8106 (2014)
18. H. Yin, X. Yang, et al., *Oncotarget* **8**, 71642 (2017)
19. H. H. Kim, S. J. Park, et al., *Biochim. Biophys. Acta.* **1854**, 449 (2015)
20. J. Wang, N. Tochio, et al., *Biochem. Biophys. Res. Commun.* **441**, 701 (2013)
21. J.-S. Hyun et al., *Journal of the Korean Magnetic Resonance Society* **22**, 149 (2018)
22. B. Kim et al., *Journal of the Korean Magnetic Resonance Society* **25**, 8 (2021)
23. M. D. Seo, S. H. Seok, et al., *Life (Basel)* **11**, 379 (2021)